

BEAM DYNAMICS STUDIES ON THE 100MEV/100KW ELECTRON LINEAR ACCELERATOR FOR NSC KIPT NEUTRON SOURCE

S. Pei[#], Y. Chi, S. Wang, G. Pei, Z. Zhou, M. Hou, W. Liu, IHEP, P. R. China
 N. Aizatsky, I. Karnaukhov, V. Kushnir, V. Mitrochenko, A. Zelinsky, NSC KIPT, Ukraine

Abstract

We designed one 100MeV/100kW electron linear accelerator for NSC KIPT, which will be used to drive a neutron source on the base of subcritical assembly. Beam dynamics studies has been conducted to reach the design requirement ($E=100\text{MeV}$, $P=100\text{kW}$, $dE/E<1\%$ for 99% particles). In this paper, we will present the progress of the design and dynamics simulation results. For high intensity and long beam pulse linear accelerators, BBU effect is one big issue; special care has been taken in the accelerating structure design. To satisfy the energy spread requirement at the linac end, the particles with large energy difference from the synchronous particle should be eliminated at low energy stage to ease the design of the collimation system and radiation shielding. A dispersion free chicane with 4 bending magnets is introduced at the downstream of the 1st accelerating section; the unwanted particles will be collimated there.

INTRODUCTION

In NSC KIPT, a neutron source based on a subcritical assembly driven by a 100MeV/100kW electron linac will be constructed. This neutron source is an ANL (USA) and KIPT (Ukraine) Joint project, and its linac will be designed and constructed by IHEP, P. R. China. The design and construction of such a linac with high average beam current and low beam power losses is a challenging technical task. Table 1 shows the main specifications.

Table 1: Main Specifications of the NSC KIPT linac

Parameters	Values	Unit
RF frequency	2856	MHz
Beam energy	100	MeV
Beam current (max.)	0.60	A
Energy spread (1σ)	1	%
Emittance (1σ)	5×10^{-7}	m*rad
Beam pulse duration	2.7	μs
Accelerating structure	$10 \times 1.336\text{m}$	Units
klystron	$6 \times 30\text{ MW}/50\text{kW}$	Units
RF pulse width	3.0	μs
RF repetition rate (max.)	625	Hz

LINAC LAYOUT

For high intensity electron linacs, both regenerative and cumulative beam break-up (BBU) effects need to be considered. In our design, the following measures are employed to suppress the BBU effects.

- 1) Applying solenoid magnetic field along the 1st

[#]pei@mail.ihep.ac.cn

accelerating structure.

- 2) Using short quasi-constant gradient accelerating structure ($\sim 1.3\text{m}$ long) to spread the dipole higher order mode (HOM) frequencies along the structure.

- 3) Increasing the accelerating gradients of the 1st and 2nd accelerating structures to enhance the beam energy boosting rate at the low energy stage as high as possible.

- 4) Decreasing the pulsed beam current to 0.6A and beam pulse length to 2.7 μs .

- 5) Introducing triplet quadrupoles at the downstream of every one or every two accelerating structures.

- 6) Adopting a better alignment with accuracy of less than 0.2 mm (1σ).

- 7) Employing beam orbit correctors to control the beam orbit close to the accelerating structures' axes as possible.

Fig. 1 shows the schematic layout of the whole linac. 6 klystrons and 10 accelerating sections are employed with a total dynamical length of $\sim 22.3\text{m}$. $\sim 10\text{kW}$ and $\sim 2\text{-}3\text{MW}$ input RF power are needed for the pre-buncher and buncher, while 16MW and 20 MW power for the 1st and 2nd accelerating structures (A0-A1), 10MW input power for each of the rest accelerating structures (A2-A9). A dispersion free chicane system located at the downstream of the 1st accelerating section was designed to collimate the particles with large energy spread.

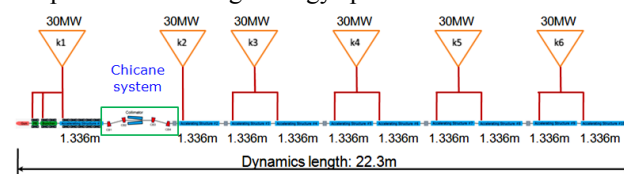


Figure 1: Schematic layout of the KIPT linac.

ACCELERATING STRUCTURES DESIGN

10 accelerating structures are employed to boost the beam energy to 100MeV. Table 2 shows the accelerating structure main parameters. To suppress the BBU (both regenerative and cumulative) effects, $\sim 1.3\text{m}$ long $2\pi/3$ mode quasi-constant gradient structure was adopted. The disk hole diameter decreases from 27.887mm to 23.726mm in a stepwise fashion along the structure (26.220mm to 19.093mm for BEPCII 3m long structure). To detune the dipole higher order modes quickly, dipole mode frequency spread was increased by increasing the average disk hole diameter step to $\sim 0.122\text{mm}$ ($\sim 0.085\text{mm}$ for BEPCII 3m long structure). At the 3rd to 6th disks of each structure, 11mm diameter holes will be drilled, by which the HEM11 mode can be increased from $\sim 4042\text{MHz}$ to $\sim 4050\text{MHz}$.

Due to the high averaged RF power loss in the linac structure, water jacket cooling is needed to sufficiently

cool down the structure. With ANSYS [1], numerical RF-thermal-structural-RF coupled finite element analysis (FEA) on the accelerating structure has been carried out. The cooling water flow rate is selected to be 10t/hour.

Table 2: Accelerating structure parameters

Parameters	Values	Unit
Operation frequency	2856	MHz
Operation temperature	40.0 ±0.1	°C
Number of cells	34+2 coupler cells	
Section length	1260 (36 cells)	mm
Cell length	34.989783	mm
Disk thickness (t)	5.84	mm
Iris diameter (2a)	27.887-23.726	mm
Cell diameter (2b)	83.968-82.776	mm
Shunt impedance (r_0)	51.514-57.052	MΩ/m
Q factor	13806-13753	
Group velocity (v_g/c)	0.02473-0.01415	
Filling time	215	ns
Attenuation parameter	0.1406	Neper

BEAM DYNAMICS

EGUN [2] and PARMELA [3] were used for the beam dynamics studies. Starting with the beam parameters at the gun exit calculated with EGUN, a 100kV/0.85A /3.85ns/3.27nC electron beam was used as an input of PARMELA to simulate and optimize the beam performance at the linac end. 10000 initial particles were used. Fig. 2 shows the beam optics in the electron gun. An electron beam with a normalized emittance of 5.264mm.mrad can be obtained at the gun exit.

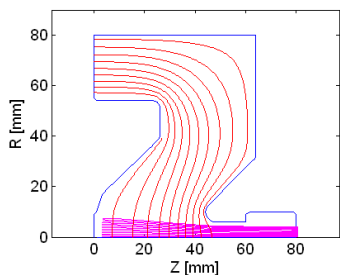


Figure 2: Beam optics for 0.85A/100kV beam.

The bunching system we used usually has a transportation efficiency of ~85%. According to our simulation, there will be ~15% particles at the downstream of the 1st accelerating structure cannot meet the 1% (1σ) energy spread requirement for 99% particles at the linac end, which will be eliminated at the low energy stage by a chicane system. The beam collimator is located between the 2nd and 3rd bending magnets to collimate the particles with large energy spread. Conclusively, the linac would have ~70% transportation efficiency (from gun to linac end). To get better beam performance, the chicane system was designed to be dispersion free by optimizing the edge angles of CB2 and CB3. ~2kW beam power will be lost in the collimator.

The beam collimation process is shown in Fig. 3, the left 4 plots are at the CB1 entrance and the right 4 plots are at the CB4 exit. Here shows the phase spectrum, beam profile, energy-phase distribution and energy spread. It can be seen from the energy-phase distribution that the particles with large energy difference from the synchronous particle are collimated successfully.

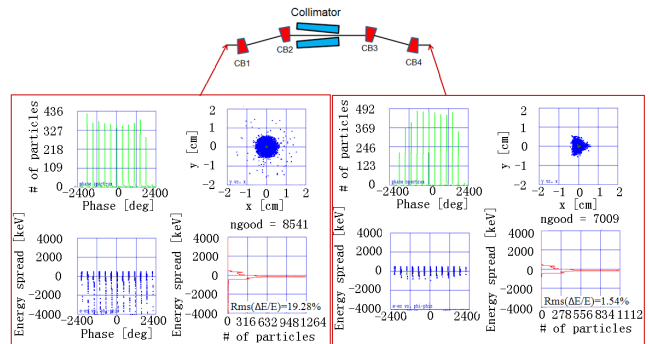


Figure 3: Beam collimation process.

Fig. 4 shows the beam bunching process, in which the longitudinal beam performances (phase spread and energy spread) at 5 locations (the gun exit, the pre-buncher exit, the buncher entrance, the buncher exit and the 1st structure A0 exit) are shown, respectively. The beam is transversely focused by ~25 solenoids from gun exit to A0 exit.

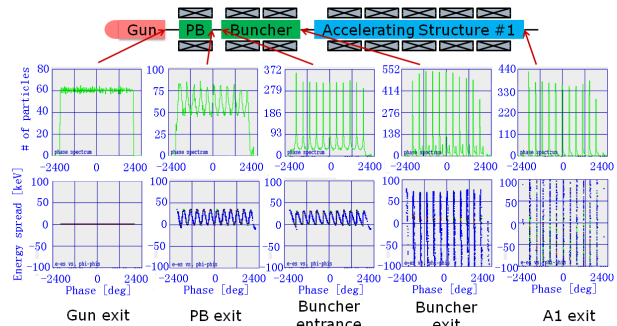


Figure 4: Beam bunching process.

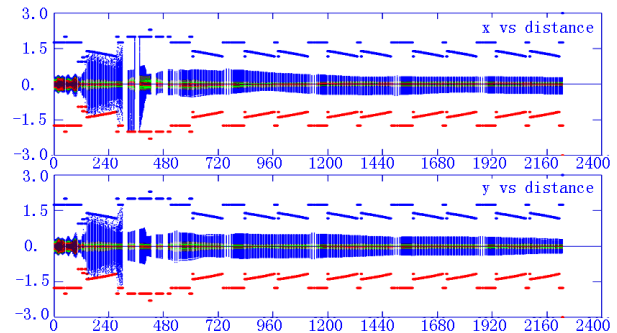


Figure 5: Beam envelopes along the whole linac (unit:cm).

Fig. 5 shows the transverse beam envelopes along the whole linac. Fig. 6 shows the PARMELA simulation results of phase spectrum, beam size, energy spectrum and energy spread from upper left to lower right at the linac end. It can be seen that the energy spread is 0.65% for 6933 good particles (99% particles of the total 7009 good particles at the linac end). The simulated 1σ

normalized emittance by PARMELA in two transverse directions is 23.4mm.mrad and 23.9mm.mrad (fairly lower than the design requirement) respectively with no any error effect considered. Even error effects (beam alignment, transverse wakefield, beam phase, etc) were considered, the total rms normalized emittance would be lower than the design requirement of 100mm.mrad. For the next step, the error effects will be studied and included.

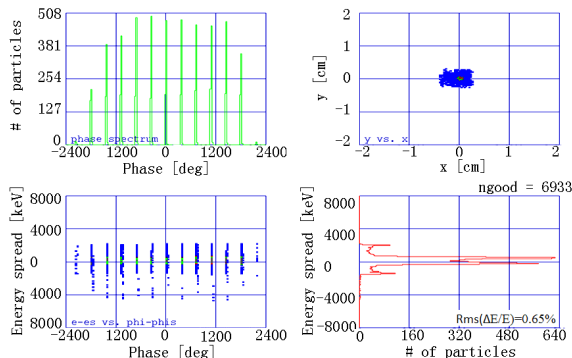


Figure 6: PARMELA simulation results at linac end.

BBU EFFECTS

The BBU calculation methodology is shown in Fig. 7. For each accelerating cell, dipole modes of the 1st six dipole bands were calculated by MAFIA [4]. For ~1.3m long structure, ~216 dipole modes were considered. Here, no solenoid magnetic field was applied. In the simulations, with or without beam orbit corrections are considered.

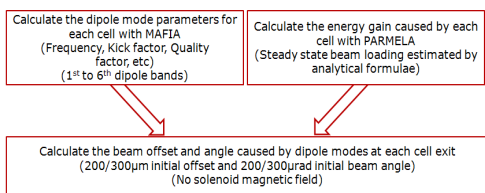


Figure 7: BBU calculation methodology.

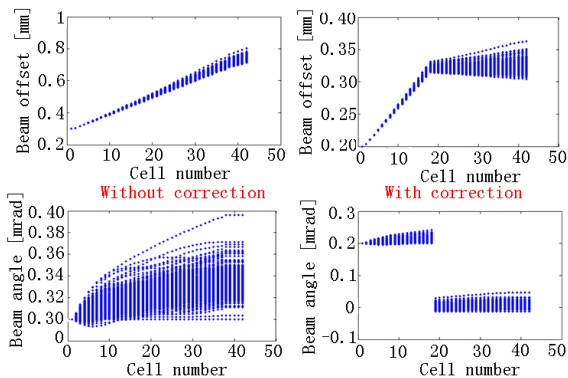


Figure 8: Beam offset and angle distribution along the 1st ~1.3m long accelerating structure.

Fig. 8 shows the beam offset and angle distribution caused by dipole modes of one 0.85A/2.7μs electron beam along the 1st accelerating structure. The left plot is

for no orbit correction case, while right is for orbit correction case. Here, +300μm and +300μrad initial beam offset and trajectory angle, which can cause the largest beam offset than the other combinations of initial offset and angle, were assumed. It can be seen that the largest beam offset caused by the dipole modes in the 1st accelerating structure is ~0.8mm without beam orbit correction and ~0.36mm with correction.

Fig. 9 shows the cumulative BBU effect calculation results. The left two plots are for no orbit correction cases, while the right two are for orbit correction cases. Here, +200μm/+200μrad initial beam offset and angle were assumed for the upper two plots, while +200μm/-200μrad for the lower two plots. If the largest beam offset is compared with the smallest aperture of the accelerating structure, it can be seen that the beam can successfully go through the linac by adopting better alignment with tolerance of less than 0.2 mm (1σ) and beam orbit correction.

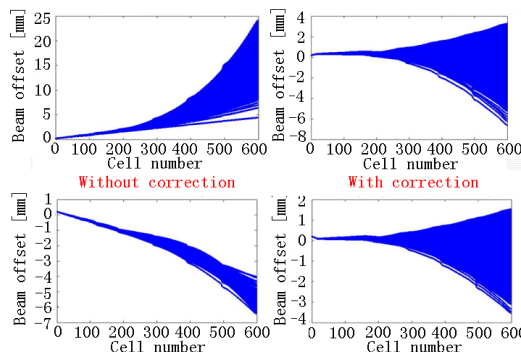


Figure 9: Beam offset distribution of one 0.85A/2.7μs beam along the whole linac.

BEAM POWER LOSS

The beam loss simulation is done with PARMELA. Fig. 10 shows the result. Most of the beam power loss located at the chicane region, where the electron beam has relatively large energy spread and ~1.7kW beam power are collimated by the collimator. The total beam power loss along the linac (from gun exit to linac end) is ~2kW, about 2% of the total beam power at the linac end.

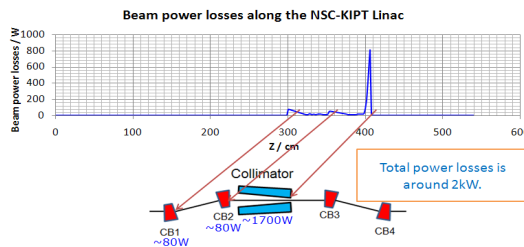


Figure 10: Beam power loss distribution along the linac.

REFERENCES

[1] ANSYS, trademark of SAS Inc., (www.ansys.com).
 [2] W. B. Herrmannsfeldt, SLAC-331, 1998.10.
 [3] L. M. Young et al, LA-UR-96-1835, LANL, 2005.7.
 [4] The MAFIA Collaboration. MAFIA User Manual version 4.106. Germany: CST Inc, 2000